LIMNOLOGY and OCEANOGRAPHY

ASLO

Limnol. Oceanogr. 67, 2022, 1805–1819

doi: 10.1002/lno.12168

Potential global distribution of a temperate marine coastal predator: The role of barriers and dispersal corridors on subpopulation connectivity

Agustín M. De Wysiecki [1*] **Federico Cortés** [2] **Andrés J. Jaureguizar** [3,4,5] **Adam Barnett** [6,7]

[1]Centro Para el Estudio de Sistemas Marinos, Consejo Nacional de Investigaciones Científicas y Técnicas (CONICET), Puerto Madryn, Chubut, Argentina
[2]Instituto Nacional de Investigación y Desarrollo Pesquero, Mar del Plata, Buenos Aires, Argentina
[3]Comisión de Investigaciones Científicas de la Provincia de Buenos Aires (CIC), La Plata, Buenos Aires, Argentina
[4]Instituto Argentino de Oceanografía (IADO), Bahía Blanca, Buenos Aires, Argentina
[5]Universidad Provincial del Sudoeste (UPSO), Coronel Pringles, Buenos Aires, Argentina
[6]Marine Data Technology Hub, James Cook University, Townsville, Queensland, Australia
[7]College of Science and Engineering, James Cook University, Townsville, Queensland, Australia

Abstract

Predicting the potential distribution of species and possible dispersal corridors at a global scale can contribute to better understanding the availability of suitable habitat to move between, and the potential connectivity between regional distributions. Such information increases knowledge of ecological and biogeographic processes, but also has management applications at a global scale, for example, for estimating the restocking ability of exploited regional subpopulations. As a case study, we tested the utility of environmental niche modeling to investigate the potential global distribution of a highly mobile temperate marine coastal species, the broadnose sevengill shark (*Notorynchus cepedianus*). First, we characterized and compared three model variants using global data and regional data from two geographically distant and genetically diverging subpopulations in the Southwest Atlantic and southern Australia. The best performing model was then transferred to the rest of the world to obtain a final global prediction for the species. Predictions revealed broad suitable areas across temperate regions of the Northern and Southern Hemispheres. As a final step, we overlaid underwater seamount data on suitability maps to simulate possible dispersal corridors and regional connectivity. Global subpopulation connectivity and dispersal are discussed in the light of recent genetic evidence, to help explain why unoccupied suitable areas are not currently accessed by the species. This study highlights the potential use of global and regional data for the assessment of habitat suitability of species at a global scale, and provides considerations when applying these models to other highly mobile species.

With greater availability of environmental, biodiversity and species distributional data at the global scale, environmental niche modeling is increasingly used in ecological studies focused on distribution and habitat use (Araújo et al. 2019). The correlative nature of niche models allows for transferability of information to other geographical spaces, providing a way for analyzing potential global distributions and habitat suitability for wide-ranging and invasive species (Battini et al. 2019). In the marine realm, regional studies applying niche model techniques are increasing exponentially (Melo-Merino et al. 2020), yet those investigating the potential global distribution of species are less common. An early example searching for potential global distribution and new subpopulations has predicted habitat suitability for the rare coelacanth fish (Owens et al. 2012). In the case of threatened marine taxa, predicting suitable areas could constitute a preliminary estimate of distribution, which could be used in a decision-making context.

The more detailed ecological information that can be incorporated into niche analyses for a species, the more skillful the distribution predictions. Such information may also contribute to better understanding the dispersal potential and the effects of marine barriers in limiting dispersal and

*Correspondence: adewysiecki@cenpat-conicet.gob.ar

Additional Supporting Information may be found in the online version of this article.

Author Contribution Statement: A.D.W. originally formulated the idea, developed methodology and models, all authors discussed results, and A.D.W. and A.B. led the writing with supporting contributions from F.C. and A.J.J.

connectivity between regional distributions. Marine barriers can both arise from a geographic discontinuity of habitats or sharp environmental gradients, for example, depth, geographic distances, or temperature and/or salinity gradients, that create physical and physiological barriers between patches of suitable habitat (Dawson 2016; Hirschfeld et al. 2021). The dispersal ability of a species, the availability of suitable habitat to move between, and the permeability of barriers (e.g., the availability of dispersal corridors) influence the likelihood of dispersal (Hirschfeld et al. 2021). In turn, this dispersal potential may affect how a species adjusts its distribution and habitat use patterns in the face of climate change. For instance, for tropical and subtropical species with advantageous dispersal potential and opportunities, warming waters can lead to an extension of their distributions (Sunday et al. 2015; Niella et al. 2022) while for temperate species warming waters could lead to contracting distributions (MacLeod 2009). The contraction of available habitat for temperate coastal species with limited potential to disperse could be particularly impactful in climate change hotspots (where water temperatures are increasing at a faster rate), if no suitable coastal areas are available to move further into higher latitudes. As an example, temperate coastal species in Tasmania, Australia, have nowhere further south to move to, so may experience compressed distributions or will need to adapt to survive in warmer coastal waters or in deeper waters (Frusher et al. 2014; Barnett et al. 2017).

The broadnose sevengill shark (*Notorynchus cepedianus*) is a widely distributed coastal associated apex predator that occurs in most temperate waters of the major ocean basins of the world. The notable exception is its absence from the North Atlantic Ocean (i.e., European and Northeast American regions, Barnett et al. 2012). *N. cepedianus* belongs to the oldest lineage of modern sharks (Hexanchiformes), with fossils dating back to the Lower Jurassic (~ 190 Mya) (Maisey 2012). Fossil evidence shows the genus *Notorynchus* was widespread in the North Atlantic (Europe) during the Lower Cretaceous (Smart 2001; Maisey 2012), before disappearing from the Upper Cretaceous, and reappearing almost 50 million years later in the Eocene (Smart 2001). The species *N. primigenius* represented the genus between the Oligocene-Pliocene (Reinecke et al. 2014), and seemed to have left the North Atlantic and Mediterranean around 4 Mya. At the global scale, patterns of genetic structure among most *N. cepedianus* subpopulations showed historical divergence and subsequent isolation between Oceania, Eastern Pacific, and South Atlantic basins (Schmidt-Roach et al. 2021), a pattern that is common to other globally distributed coastal shark species (Benavides et al. 2011; Bester-van der Merwe et al. 2017). However, genetic connectivity within individual ocean basins was evident, and individual sharks can travel up to 1800 km implying highly mobile behavior and large regional displacements (Barnett et al. 2011; Williams et al. 2012; Larson et al. 2015). Although *N. cepedianus* is capable of large scale movements, transoceanic dispersal may not occur (which information to date suggests) because of the species' benthic habitat association (Barnett et al. 2010*a*) with engrained coastal habitat use patterns, combined with high fidelity to feeding grounds (Barnett and Semmens 2012; Irigoyen et al. 2018).

N. cepedianus occurs in high abundance in a number of coastal regions (Barnett et al. 2012), for example, in the west coast of the USA (Ebert 1989; Williams et al. 2012), in Patagonia, Argentina (Lucifora et al. 2005; Irigoyen et al. 2018), in Namibia and South Africa (Ebert 1996; Engelbrecht et al. 2020), Tasmania, Australia (Barnett et al. 2010*b*), and New Zealand (Lewis et al. 2020). Its presence has also been reported in Chile (Bustamante et al. 2021), Japan (Tanaka et al. 2013), Taiwan (Ebert et al. 2013), Tristan da Cunha Islands (Caselle et al. 2018), and Galápagos Islands (Buglass et al. 2020), although only limited records for those areas. Site fidelity to specific coastal habitats (Ebert 1996; Barnett et al. 2011; Irigoyen et al. 2018) and large-scale movements have been reported for the species (Barnett et al. 2011; Williams et al. 2012; Stehfest et al. 2014). Recently, using environmental niche theory, the potential distribution of *N. cepedianus* in the Southwest Atlantic was investigated (De Wysiecki et al. 2020). A migratory pattern characterized by two main north–south seasonal displacements was inferred, with distance to coast, surface water temperature, and turbidity gradients as important drivers of distribution (De Wysiecki et al. 2020). The global vulnerable conservation status of *N. cepedianus* (Finucci et al. 2020), the recent regional declines in abundance (Barbini et al. 2015; Irigoyen and Trobbiani 2016), and its ecological importance and wide distribution (Barnett et al. 2012) highlight this species as an ideal case study to model its potential global distribution as a prerequisite for developing regional conservation management strategies.

The objective of this study is to investigate the potential global distribution of *N. cepedianus*. Because of the coarse nature of this objective and fragmentary availability of global presences and absences of the species, we use a presence-only ecological niche modeling approach. Ecological niche models are used to determine potentially suitable habitats for the species across the world. To determine the best niche transfer scenario, we compared three model fits considering the global population of the species (global fit) or subpopulations in the Southwest Atlantic and southern Australia (regional fit, both merged and individual variants), where comprehensive presence-only data were available. The global fit is intended to model the full niche of *N. cepedianus* global population (i.e., existing realized niche, Hutchinson 1957; Peterson et al. 2011), whereas the regional fit is intended to model subpopulation niche patches as samples of the full niche. Three model variants were implemented because the species shows high basin-scale connectivity but weak transoceanic connectivity, and because available presence data representative of the global population are fragmentary. The regional fit of individual subpopulations further allowed us to compare habitat

use between two distant and diverging regional distributions of *N. cepedianus*. Finally, by mathematically simulating possible dispersal corridors, we examine opportunities for regional connectivity and why unoccupied suitable areas are not currently accessed by the species.

Materials

An environmental niche modeling approach was used to predict (continuous and binary) annually averaged habitats suitable for *N. cepedianus* in the different regions of the world. Conceptually, we framed our analysis in the Eltonian Noise Hypothesis, which is based on the assumption that at coarse-grained scales (i.e., geographic scales), climatic variables (also termed "scenopoetic") fundamentally shape the niche, whereas biotic interactions represent a "noise" and their effects may be averaged-out (Soberón and Nakamura 2009). This is particularly relevant for species with a generalized diet and limited predators as *N. cepedianus*. First, best global and regional distribution data points were used to characterize the full population niche and subpopulation niche patches of two geographically distant subpopulations of *N. cepedianus* in the Southwest Atlantic and southern Australia (De Wysiecki et al. 2020; A. De Wysiecki unpubl. data). The final models were then transferred to the rest of the world, and their performance compared to obtain the best global prediction for the species. Temporally explicit modeling was not attempted as presence data were too sparse at sub-annual timescales to fit models.

To promote transparency and reproducibility, we describe the methodological approach following the Overview, Data, Model, Assessment, Prediction (ODMAP) protocol for species distribution models (Zurell et al. 2020). A complete overview of methods is formulated here as a text flow, but a detailed description of the five ODMAP sections can be found in Supplementary Information. All analyses were developed with R version 4.1.2 (R Core Team 2021), and code is available on GitHub (Agustindewy/Sevengill_shark_global).

Presence-only data

Global *N. cepedianus* presence data were obtained from the available published literature and biodiversity repositories. First, a literature review was conducted in Google Scholar using the terms "*Notorynchus cepedianus*" and "*Notorynchus*" to identify peer-reviewed and gray literature articles reporting *N. cepedianus* presences across the different regions of the world (Supporting Information). When only the location of the presence was reported, we manually georeferenced the presence record. Second, *N. cepedianus* presence data were downloaded from the Global Biodiversity Information Facility (GBIF 2020) and the Ocean Biodiversity Observation System (OBIS 2020) repositories. Biodiversity repository data were cleaned following recommended practice, including the removal of duplicates, presences with missing/odd coordinates or on land, and environmental outliers (Cobos et al. 2018). For a greater representation of presence data in the Southwest Atlantic and southern Australia, we also collected additional freely accessible records from social media (Facebook posts, details on how these data were collected in De Wysiecki et al. (2020)), and the New South Wales Shark Meshing Program. Although *N. cepedianus* in Australia was well represented by the data (A. De Wysiecki unpub. data), the freely accessible records in the Southwest Atlantic did not fully represent its known distribution (De Wysiecki et al. 2020). Therefore, additional records from historical research cruises and observer programs were requested from the Instituto Nacional de Investigación y Desarrollo Pesquero (INIDEP, Argentina). Records prior to the year 1900 were disregarded for calibration. Overall, we retained a total of 1068 *N. cepedianus* presence records worldwide after data cleaning, resulting in a temporal span between the years 1904 and 2020 (1907 and 2019 for the Southwest Atlantic; 1904 and 2020 for southern Australia). The majority of these records are freely available and compiled in Supporting Information.

Models

Calibration data

The cleaned presence data set corresponding to the global known distribution of *N. cepedianus* was used for model calibration. To feed the three model calibration variants, presence data were split in a global set ($n = 1068$), a regional merged set ($n = 706$, Southwest Atlantic and southern Australia), and two regional individual sets ($n = 312$, Southwest Atlantic; $n = 394$, southern Australia). To reduce the spatial clustering of calibration sets, we applied a thinning distance of 50 km in both regions ("spThin" R package, Aiello-Lammens et al. 2015). This distance was chosen based on the visual inspection of regional presence records which were increasingly thinned (10 km increments) until spatial clusters in the data were successfully reduced (Supporting Information Figs. S1, S2). In addition, we applied an environmental filter to reduce the effects of sampling bias and clusters of data in environmental space, using the "envSample" custom function, 0.5°C sea surface temperature and 1 km distance to the coast filter values (Varela et al. 2014).

Calibration area

For each of the three modeling variants, we define accessible areas based on 1000 km buffer polygons around every calibration record to determine the calibration area (i.e., M space, Soberón and Peterson 2005). This buffering distance was chosen based on acoustic and satellite tracking data, which shows that *N. cepedianus* is capable of performing at least 1000 km long-scale movements (Barnett et al. 2011; Stehfest et al. 2014). There is evidence that *N. cepedianus* can cover longer distances (~ 1800 km, Williams et al. 2012); however, this occurred within the core area of its distribution and buffering areas that large are unlikely to represent accessible areas across

the perimeter of its distribution. The calibration area was used to randomly select background data (n = 10,000) for model calibration.

Environmental data

Based on previous studies on the species (Ebert 1989; Barnett et al. 2012; De Wysiecki et al. 2020) and environmental factors known to influence large-scale habitat use of other sharks and rays (Schlaff et al. 2014), we only considered relevant predictor variables as the potential set of environmental conditions that allow *N. cepedianus* to maintain its subpopulations. Five of these variables described the surface water and water column. The sea surface temperature, mean temperature at mean depth, and mean salinity at mean depth indicate the physiological limits of the species (Stehfest et al. 2014). The diffuse attenuation coefficient Kd490 indicates coastal turbid areas, seasonally associated with observed species presences (De Wysiecki et al. 2020). The primary productivity is a proxy for productive areas with greater food availability. A sixth predictor was considered, the chlorophyll *a* concentration, but showed high correlation ($r > 0.7$ Pearson correlation, Dormann et al. 2013) with the coefficient Kd490 across the full study area and was discarded to avoid multicollinearity.

Two more predictors, the bathymetry and slope, were considered to describe topography. Both predictors showed important differences in their range values between the Southwest Atlantic and southern Australia. To explore these differences, we compared a simplified version of the two subpopulation habitat patches based on ellipsoids (method description in Section "Niche comparison"). This exploratory analysis showed that the southern Australia coastal habitats include unexpected extreme depth and slope values compared to those in the Southwest Atlantic (Supporting Information Fig. S3). In southern Australia, however, evidence suggests that *N. cepedianus* is caught at depths down to 530 m (99.9% quantile, AFMA's logbook data, unpubl. data), whereas the same catch location corresponds to areas as deep as 3860 m in the bathymetry raster. This discrepancy between depths measured on site and depths derived from bathymetric models may be related to confounding effects that occur at the edge of *N. cepedianus*' distribution across the steep slopes of the continental shelf margin. Because the slope raster is derived from the bathymetry raster, we attributed the discrepancy to the same confounding effects. As a result, we replaced these two variables with the distance to the coast to prevent estimating too broad environmental tolerances for the species (Supporting Information Figs. S3, S4). The distance to the coast predictor describes the distance to important coastal habitats (i.e., parturition, nursery, and feeding grounds) key to the survival of the species.

The oceanographic variables, including bathymetry, were downloaded from the global Bio-ORACLE marine dataset (version 2.1), at a resolution of ~ 5 arcmins and a global extent (Assis et al. 2018). The distance to the coast was downloaded from the Global Self-consistent, Hierarchical, High-resolution Geography Database (version 2.3.7), at a resolution of ~ 1 arcmins and a global extent (Wessel and Smith 1996). The slope of underwater terrain was constructed from the bathymetry raster using the *terrain* function in the "raster" R package (Hijmans 2021). The distance to the coast variable was resampled to ~ 5 arcmins using the *aggregate* function in the "raster" R package. The final raster layers (n = 6) were masked by the calibration areas prior to variable selection and modeling. To integrate the sparse data and nonrepeated sampling over time, we treated presence observations irrespective of the year of sampling as a presence. Our temporal data binning was motivated by the fact that environmental data on oceanographic variables had a native coverage from 2000 to 2014, which could not match the species' sampling data ranging from 1904 to 2020. While our aggregation comes at a loss of temporal detail, it allows us to consider all presence data available.

Ecological niche modeling

For each modeling variant, we applied the MaxEnt algorithm (version 3.4.3, Phillips et al. 2006) based on the automated calibration and evaluation protocol implemented in the 'ENMeval' R package, version 2.0.3 (Muscarella et al. 2014; Kass et al. 2021) for comparing candidate models of differing complexity. We considered the subset of feature classes that yield the simplest linear and bell-shaped responses (i.e., linear + quadratic, linear + product, and linear + quadratic + product) and a complete set of regularization multipliers (i.e., sequence from 0.1 to 2 by 0.1 increments, plus 2.5, 3, 4, 5, 7, and 10); that is, 78 candidate models. This protocol allows selecting the most significant (partial area under the receiver operating characteristic, pROC), and best-performing 10% omission rate threshold) (Cobos et al. 2019*b*). Best parameterizations that met the selection criteria were used to create final models and to predict habitat suitability over the calibration area.

To test the ability of models to extrapolate to new areas and to reduce the spatial autocorrelation, the calibration records and background points were partitioned into spatial blocks grouped in bins (k = 5) for k-fold cross-validation during the ENMeval run. During this evaluation process, one bin is used for testing and the remaining ($k - 1$ bins) for model fitting in an iterative way until all the bins have been used for testing (Valavi et al. 2019). The effective block size over which observations are spatially independent and the spatial blocks were determined with the *spatialAutoRange* and *spatialBlock* functions from the "blockCV" R package, respectively (Valavi et al. 2019). We used the continuous Boyce (CBI) index as a final comparison of predictions against observed truths to statistically decide which model variant was best for global transfers (Hirzel et al. 2006; Leroy et al. 2018).

We used an exhaustive approach for variable selection to determine the best combination of variables for modeling

because it has been shown to prevent both underfitting and overfitting of geographic projections compared to other standard approaches (Cobos et al. 2019*a*). The approach consists of modeling all variable combinations and evaluating them comparatively to decide which is best suited to describe the niche, avoiding suboptimal choices. Because the number of possible combinations (i.e., 6 predictors, 63 combinations) would make the analysis challenging (i.e., 63 combinations times 78 different model complexities = 4914 candidate models), we fixed sea surface temperature, diffuse attenuation coefficient and distance to coast because these predictors were important in shaping the niche of *N. cepedianus* in the past (De Wysiecki et al. 2020). This choice narrowed down possible combinations to eight. In addition, the analysis was done considering a coarse set of regularization multipliers (i.e., 0.1, 0.5, 1, 2.5, 5) using the kuenm protocol (i.e., 8 combinations times 15 different model complexities = 120 candidate models) and was applied only to the global variant because it is the one including all available data.

Global prediction

Final global and regional models were then transferred across the globe, with the exception of the Arctic and Antarctic territories. This allows us to predict broad regions of the world potentially suitable for *N. cepedianus* in geographic space. Strictly extrapolated areas were disregarded based on the mobility oriented parity analysis (Owens et al. 2013). A binary prediction was also created based on 10% and 5% minimum training presence, which are the thresholds finding the lowest predicted suitability values for 90% and 95% of presence points, respectively. Binary cut-off values are useful for interpreting probabilistic predictions and sensitivity of results. In the case of the regional individual fits, a single final global prediction was created as an ensemble mosaic between the two individual predictions, keeping the median value in each pixel.

Subpopulation niche comparison

We performed a habitat overlap test to statistically decide whether the subpopulation niches of *N. cepedianus* in the Southwest Atlantic and southern Australia overlapped or not. The test models the environmental niche as ellipsoids considering the availability of conditions for each subpopulation (i.e., relevant conditions), as opposed to the full set of conditions (background test in "ellipsenm" R package; Cobos et al. 2020). Ellipsoids were estimated as minimum volume ellipsoids based on an algorithm designed to reduce the volume to a minimum while covering all presence data falling within a breakdown value, reducing the effect of outliers in environmental space. The breakdown value is defined as the smallest percentage of contamination that can have an arbitrarily large effect on the niche (Van Aelst and Rousseeuw 2009). An observed overlap value is first calculated as the proportion of overlapping points between the model ellipsoids of the two niches. Then, the observed overlap is compared with the frequency distribution of values scored across 1000 Monte-Carlo replicates constructed from randomly sampling the background with a sample size equal to the number of presence records, and creating an ellipsoid model in each case. If the observed value falls within the 95% confidence interval, the null hypothesis of niche overlap cannot be rejected.

Connectivity assessment

Based on the different degrees of genetic isolation between global subpopulations of *N. cepedianus* (Schmidt-Roach et al. 2021), we were interested in testing whether seamounts and knolls may facilitate their connectivity via stepping stone-like dispersal corridors. We assumed that buffer areas around seamounts may provide temporary demersal habitat suitability during rare events of drifting individuals from coastal areas, allowing them to surpass warm thermal barriers and oceanic pelagic environments. Seamount and knoll base polygon data (Yesson et al. 2011) within the known depth range of the species (i.e., < 600 m deep) were first overlaid to habitat suitability maps. We used 80 km buffer areas around seamount centroids because this is the estimated distance *N. cepedianus* can travel at average cruising speed per day (i.e., 0.99 m s^{-1}, Barnett et al. 2010*a*). We also assumed that expected habitat suitability around seamounts proportionally increased to their centroids from the minimum to the maximum value predicted in the final niche model. Dispersal through waters exceeding the lower temperature tolerance of the species (i.e., subantarctic/subarctic regions) or transoceanic dispersal was considered as not possible.

The final global raster of compound habitat suitability (environmental niche + seamount buffers) was used along with global presences to evaluate connectivity plausibility between occupied regions, and from occupied regions to invadable areas. The plausibility of potential dispersal was assessed through the dispersal simulations implemented in Nuñez-Penichet et al. (2021) via the bam R package (Osorio-Olvera and Soberón 2020). The simulation starts at occupied cells (i.e., presence records) from which adjacent cells can be visited by the species, and be occupied if suitable. In each time step, the possibility of reaching neighboring cells is determined by a connectivity matrix that defines clusters of cells connected by dispersal (detailed procedures available in Nuñez-Penichet et al. (2021)). To account for sensitivity in the analysis, we explored (i) a set of 10 different dispersal parameters (1–10 adjacent cells per unit of time) which determine how far the species is able to move in one unit of time (i.e., 10–100 km dispersal a day), and (ii) a set of 10 different minimum training presence thresholds (1% to 10%) used to create the binary suitable maps. Two hundred time steps (days) were allowed in each simulation to ensure steady results. A total of 100 simulated layers (10 parameters by 10 thresholds) are then summed up to visualize the final simulation results. A score of 100 in a

cell indicates 100% occupation in that cell, whereas a value of 0 means that the species never occupied that cell. A connection was considered plausible only when clear corridor-like suitable patches occurred between regions. Instead of one simulation with a global extent (computationally limiting), simulations were performed only across the relevant dispersal corridors within major oceanic basins.

Results

Calibration of models

The number of calibration points retained after the spatial and environmental filtering, as well as the calibration areas varied between the three model variants (Table 1; Supporting Information Fig. S5; calibration points in Supporting Information). The variable selection process selected all six environmental variables as the optimal combination of predictors to describe the niche with a global fit (pROC = 0, $OR_{10\%}$ = 0.047, ΔAICc = 0). The global fit outperformed both regional fits indicating a greater ability to predict the species presence globally (Table 1). The global model predictions across the calibration area indicated highest habitat suitability over coastal (< 250 km) and turbid areas (optimal ~ 0.25 m^{-1}) with optimal values of surface temperature of ~ 15°C and mean depth temperature of ~ 13°C (Supporting Information Fig. S6). In contrast, distant areas from the coast were less suitable for the species.

Global prediction

The final predictions based on the global fit revealed broad potentially suitable areas for *N. cepedianus* across temperate regions of the Northern and Southern Hemispheres (Fig. 1; continuous predictions in Supporting Information Fig. S7; regional and three-predictor predictions in Supporting Information Fig. S8). These regions included the Northwest, Northeast, and Southeast Pacific, Northwest, Northeast and Southeast Atlantic,

Table 1. Parametrization of best-selected models for *Notorynchus cepedianus* global population and subpopulations in the Southwest Atlantic and southern Australia. The models were selected after three-step criteria based on the partial area under the receiving operator characteristic (pROC), 10% threshold omission rate ($OR_{10\%}$), and continuous Boyce index (CBI).

Model fit	Calibration points	Feature classes	Regularization multiplier	Selection criteria			Number of parameters
				$OR_{10\%}$	pROC	CBI	
Global	255	lq	0.1	0.011	0.000	0.894	12
Regional merged	172	lq	0.1	0.048	0.000	0.703	12
Regional independent							
Southwest Atlantic	80	lq	0.1	0.097	0.000	0.827	12
Southern Australia	96	lqp	0.3	0.022	0.000	0.776	23

lq = linear + quadratic; lqp = linear + quadratic + product.

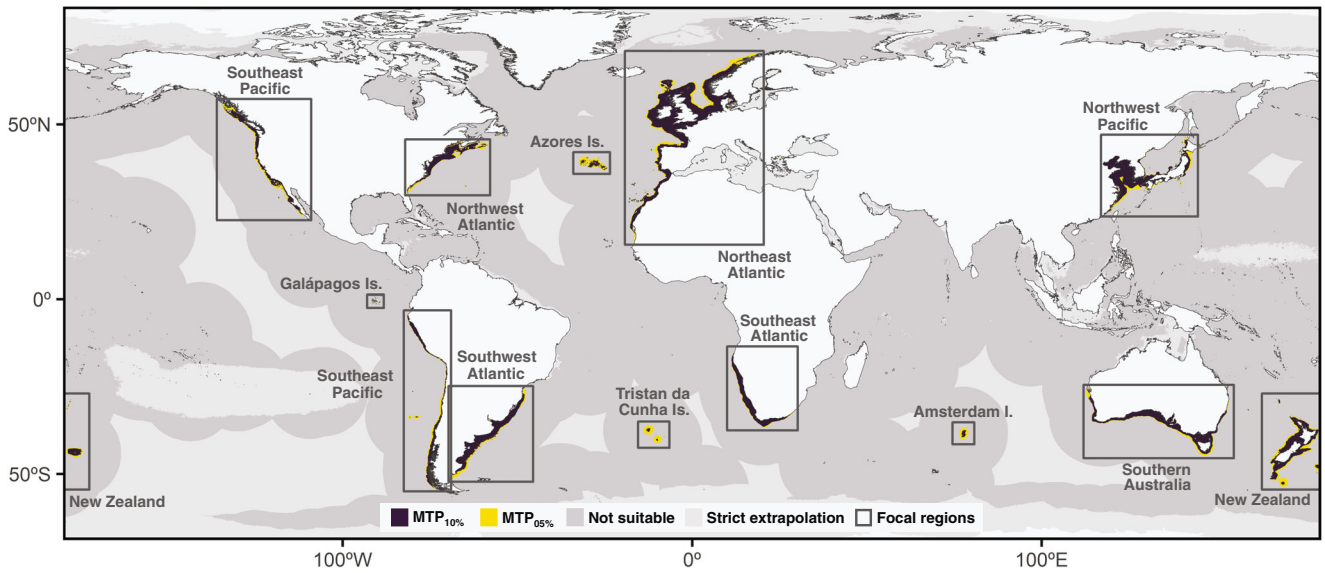

Fig. 1. Global predictions of binary habitat suitability for *Notorynchus cepedianus*. Suitability is expressed as the 10% and 5% minimum training presence thresholds. The different broad regions with predicted suitable areas are named and delimited as focal regions.

New Zealand, and four offshore islands (Azores, Tristan da Cunha, Galápagos, and Amsterdam/Saint-Paul). Based on known distribution presences, the broad suitable regions occupied by *N. cepedianus* are the Northwest, Northeast and Southeast Pacific, Southwest and Southeast Atlantic, Australia and New Zealand (Fig. 2). The Northwest and Northeast Atlantic continental regions represented potentially suitable areas in which *N. cepedianus* does not currently occur or has not yet been detected (Supporting Information Fig. S9). In the case of offshore territories, Tristan da Cunha and Galápagos Islands were the only suitable regions for which reports of *N. cepedianus* exist in the literature (Supporting Information Fig. S10).

Subpopulation niche patches

N. cepedianus niches from Southwest Atlantic and southern Australia subpopulations were less similar than expected at random when comparing them based on minimum volume ellipsoids (overlap = 0.186, *p*-value = 0; Fig. 3a,b). Ecological distinctiveness between habitat patches resulted from sharks occupying colder environmental conditions in the Southwest Atlantic than southern Australia (Fig. 3a; Supporting Information).

Dispersal corridors

Based on predicted habitat suitability and global presences presented in the previous sections, dispersal corridors within

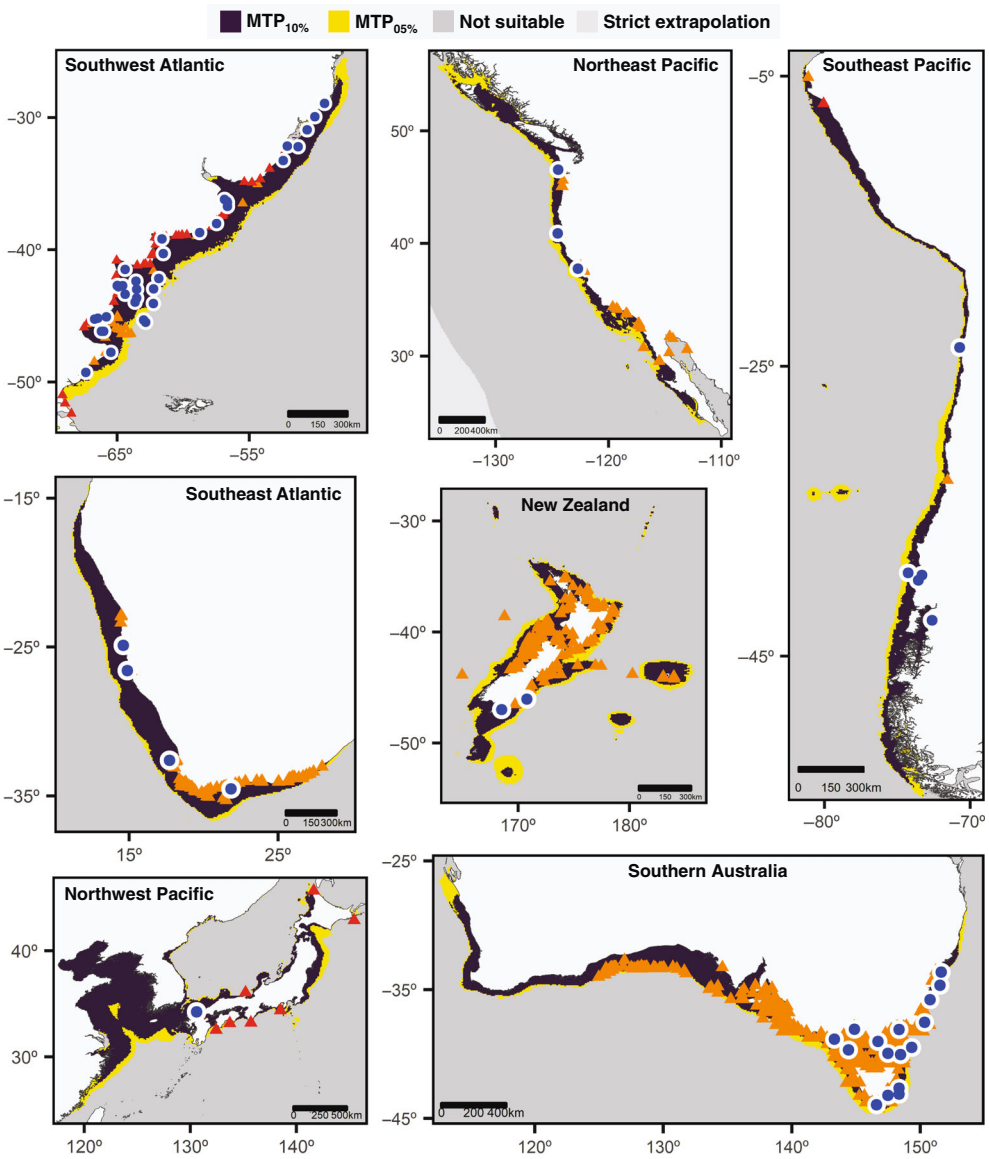

Fig. 2. Binary habitat suitability for *Notorynchus cepedianus* in continental regions of the world predicted as suitable and where the species has been reported to occur based on published literature (blue dots). Suitability is expressed as the 10% and 5% minimum training presence thresholds. The delimitation of the regions corresponds to the regions shown in Fig. 1. The locations of freely available records are also indicated, that is, biodiversity repositories (orange triangles) and other records from gray literature and social media (red triangles). Note that institutional records in the Southwest Atlantic are not shown because they are not freely available.

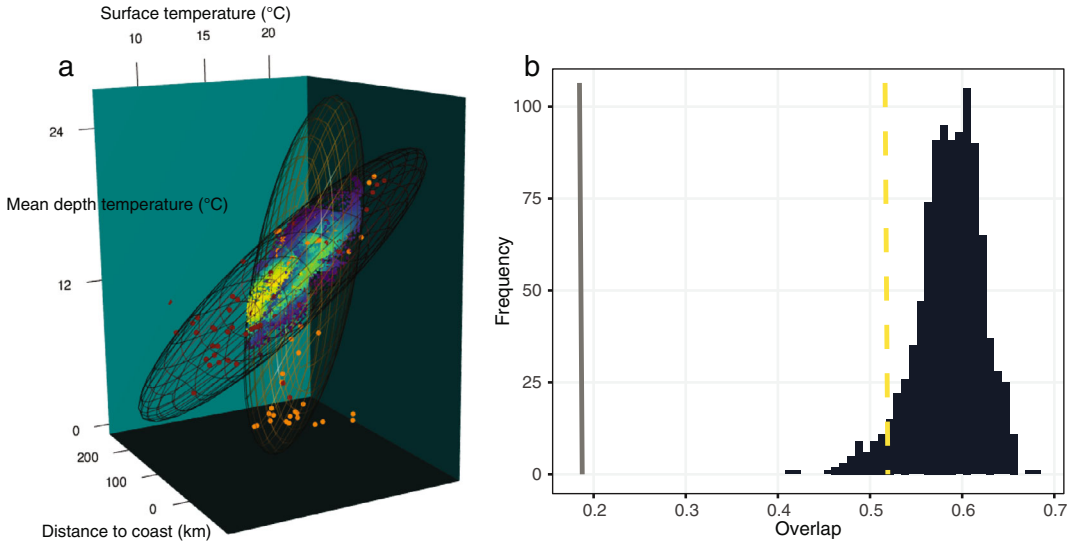

Fig. 3. Background overlap in environmental space between the ecological niches of *Notorynchus cepedianus* subpopulations in the Southwest Atlantic (SWA) and southern Australia (AUS). (**a**) Minimum volume ellipsoid representation of niches (three most important predictors in models; SWA = red, AUS = orange), including species data (dots) and background points (color scale with lighter colors toward the center of the SWA ellipsoid). (**b**) Statistical test results for the observed overlap (solid line) and 5% confidence limit (dashed line) of the frequency distribution of 1000 Monte-Carlo simulations constructed from randomly sampling the background with an *n* equal to the number of records for each niche (using all predictors).

three major ocean basins may facilitate basin-scale subpopulation connectivity, namely the East Pacific, South Atlantic, and Oceania. Dispersal simulations using the compound habitat suitability between the final niche model and seamount buffers indicated plausible connection through underwater seamounts and knolls between Southeast Pacific and both Galápagos and Juan Fernández Islands (Fig. 4a,b), Southeast Atlantic and Tristan da Cunha Islands (Fig. 4c), and southern Australia and New Zealand (Fig. 4d). Conversely, no plausible connection resulted between the Southwest Atlantic and Tristan da Cunha Islands (Fig. 4e), Northeast Pacific and Galápagos Islands (Fig. 4a), or from the Northwest Pacific to any other region (Fig. 4e). In addition, dispersal from South Atlantic subpopulations to suitable predicted (invadable) areas of the North Atlantic Ocean was not plausible (Fig. 6c,e). Connectivity between the Southwest Atlantic and Southeast Pacific (i.e., through the Magellan strait or Beagle Channel) is also considered not possible because of thermal barriers.

Discussion

This study presents a global map and assessment of the potential distribution of *N. cepedianus*, and highlights that this modeling approach might be appropriate for other highly mobile marine animals for which there is enough information on global or regional distributions for one or more subpopulations (in the case of *N. cepedianus*, the Southwest Atlantic and southern Australia). Maps confirm the potential distribution across the five broad regions of the Northeast Pacific, Southwest and Southeast Atlantic, southern Australia, and New Zealand, regions in which studies suggest *N. cepedianus* occurs in high abundance. Results also reproduce the distribution across data-poor regions for which only a few individuals have been reported, namely Chile (Bustamante et al. 2021), Japan (Tanaka et al. 2013), Taiwan (Ebert et al. 2013), Tristan da Cunha (Caselle et al. 2018), and Galápagos Islands (Buglass et al. 2020). The maps suggest that doubtful (unconfirmed) records of the species in India (Froese and Pauly 2019), are likely not valid.

The comparative analysis of the niche patches showed ecological distinctiveness between the Southwest Atlantic and southern Australia subpopulations, which resulted from sharks occupying colder environmental conditions in the Southwest Atlantic. Possible explanations for this variation may include the geomorphological differences between the two regions. Suitable coastal areas in the Southwest Atlantic extend over a geographically wider latitudinal range, as opposed to those in southern Australia, where no coast is available beyond southern Tasmania, but the coastline extends over a wider longitudinal range. Accordingly, the geographical extent of presences differed markedly between regions, being broader in latitude in the Southwest Atlantic (Southwest Atlantic = ~29°S–52°S, southern Australia = ~33°S–44°S) and broader in longitude in southern Australia (southern Australia = ~125°E–152°E, Southwest Atlantic = ~49°W–69°W). As a result of these geomorphological differences, accessible coastal areas for *N. cepedianus* in southern Australia occur over a narrower temperature range than in the Southwest Atlantic. This may cause *N. cepedianus* in southern Australia to inhabit, on average, warmer coastal waters compared to individuals in the Southwest Atlantic.

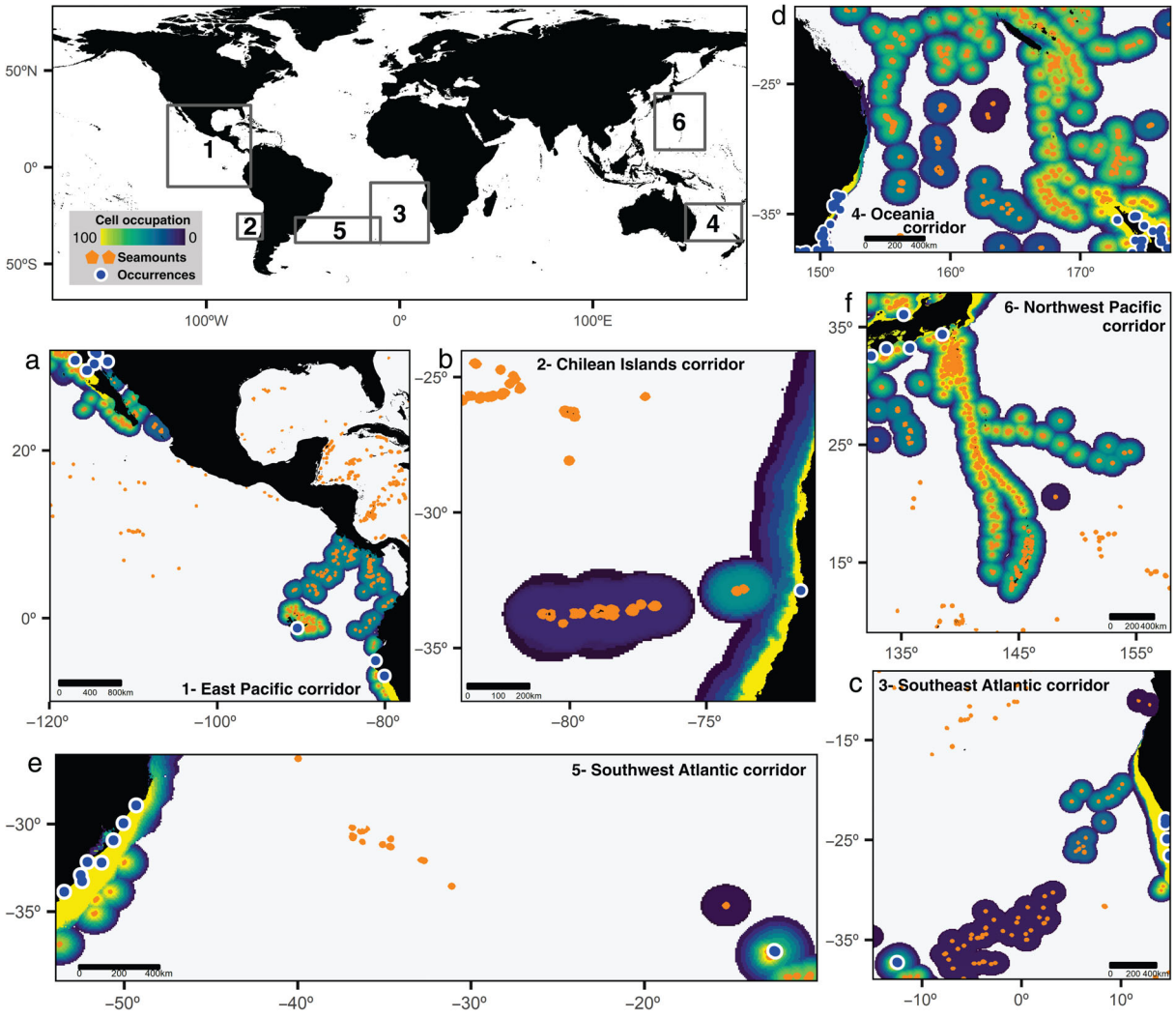

Fig. 4. Simulation results of the potential dispersal routes of *Notorynchus cepedianus* subpopulations via seamount corridors (numbers). The degree of cell occupation indicates the areas that the species commonly (lighter colors) or rarely (darker colors) reached in simulations. (**a**) East Pacific corridor (Northeast Pacific—Galápagos Islands—Southeast Pacific), (**b**) Chilean Islands corridor (Juan Fernández Islands—Southeast Pacific), (**c**) Southeast Atlantic corridor (Southeast Atlantic—Tristan da Cunha Islands), (**d**) Oceania corridor (Australia—New Zealand), (**e**) Southwest Atlantic corridor (Southwest Atlantic—Tristan da Cunha Islands), and (**f**) Northwest Pacific corridor.

Furthermore, southeast Australia (the core habitat/distribution for *N. cepedianus*) is a hotspot for climate change (Frusher et al. 2014) and therefore *N. cepedianus* may have no choice but to inhabit warmer waters or compress their distribution over time. Conversely, the Río de la Plata outer area and inner-mid shelf waters of Argentina, which are part of the *N. cepedianus*' core distribution within the Southwest Atlantic, are also a hotspot for climate change (Franco et al. 2020), but further coastal waters to the south may allow the southward expansion of its distribution over time.

It is also possible that differences between subpopulation niches are a result of assigning annual temperature values to presences that only occurred seasonally (or monthly) across the edges of the distribution (i.e., areas of vagrancy, Ingenloff and Peterson 2021). This is particularly relevant for highly mobile species like *N. cepedianus* that undertake large-scale movements and show marked migratory patterns (Barnett et al. 2011; Williams et al. 2012; De Wysiecki et al. 2020). For example, habitat use by *N. cepedianus* in the Southwest Atlantic extends to highest latitudes during austral summer (February–March), when water temperature increases in those areas (De Wysiecki et al. 2020). In this sense, overlapping distribution predictions from Southwest Atlantic and southern Australia models would represent the core distribution of the species, whereas the individual contribution of these regions to prediction may only represent the conditions at the edge of the distributions as an artifact of assigning averaged environmental values to predictors that are intrinsically dynamic. This suggests that modeling without considering temporal variation in habitat use and environmental conditions could affect

niche overlap results between distant subpopulations. Although the necessary data to include a temporal component to the analysis were not available for the study regions this needs to be considered when applying these models to highly mobile species. Temporally explicit, regional studies may clarify if the observed differences are explained by annual (average) habitat parameters or indicate true variation in habitat use between subpopulations of the same species.

Based on their limited depth range and association with temperate turbid coastal habitats, the map predictions presented in this study depict a coarse representation of the global potential distribution of *N. cepedianus*. At the regional scale, the maps serve as a preliminary yet simplified delineation of the potential distribution within each region. Therefore, describing *N. cepedianus* niche based on temperature, turbidity and distance to the coast likely fits the purpose of capturing habitat suitability that is common to all regions. However, regional habitat use patterns are likely context dependent, with other environmental and physical predictors such as oceanographic regimes, geomorphological features, and biotic determinants, relevant to the purpose of better describing the niche regionally. The discrepancy observed between the niches of Southwest Atlantic and southern Australia when including depth or slope as a predictor illustrates this point and suggests that bathymetry is relevant regionally. For example, the records compiled in this study for New Zealand fall within the complex-shaped polygon depicted by the 1000 m isobath, agreeing with maximum depth records (~ 550 m) for the species in the region (see *N. cepedianus* figure in Anderson et al. (1998)) and indicating a corridor between the South Island and Chatham Islands. Other variables potentially important regionally for *N. cepedianus* include the distance to thermal fronts and prey, such as pinniped colonies (De Wysiecki et al. 2020). It is increasingly recognized that habitat use by coastal marine taxa is context dependent at various scales (Bradley et al. 2020). Therefore, future modeling considering the regional physical context may help determine the relevance of different habitat types for more applied regional outcomes.

The presence data used for the analysis were obtained from a variety of sources, including published literature, and freely available sources such as biodiversity repositories (and sources within) and social media. However, while free-access avenues were key contributors to niche studies, care must be taken when considering these data as they can be incomplete and/or biased (Hortal et al. 2008). This is particularly relevant for the study of fish because fishery-dependent and independent government fisheries research data usually have the broadest representation of species' presence (Braccini et al. 2020), but these data have confidentiality agreements in place and are therefore difficult to access. For example, freely accessible data for the Southwest Atlantic alone barely represented the full distribution of *N. cepedianus* in the region and additional data from the Argentinian government was central to the analysis. In the case of southern Australia, a dataset from the former Bureau of Rural Sciences within biodiversity repositories provided a uniquely broad representation of the species' geographical extent in the region. Failing to consider a broad and more realistic representation of the species' presence in geographical space may lead to limited understanding of their niche. In this regard, the copious free data compiled in this study for the Northeast Pacific, Southeast Atlantic and New Zealand regions may have potential use in combination with official government data for more comprehensive regional studies of *N. cepedianus* subpopulations.

Galápagos Islands were the only region in which *N. cepedianus* occurs but was only marginally predicted as suitable habitat. Their presence was reported for the first time only recently (Buglass et al. 2020), as two individuals were recorded on deep-sea cameras at a depth of 210 m during October–November (Buglass et al. 2020). Although *N. cepedianus* records in offshore islands are not new (e.g., Tristan da Cunha Islands, Caselle et al. 2018), their presence in tropical latitudes expands our knowledge of the global geographical distribution of the species. However, as Buglass et al. (2020) discussed, no sightings in the protected coastal waters of the Galápagos Islands have been reported to date, despite decades of recreational and research diving activities. This pattern of temperate water species occurring in deep but not shallow waters within a tropical or warm-temperate region is new for *N. cepedianus* ecology and suggests habitat use of cooler deep waters in tropical regions, possibly facilitated by cold currents during cold months of the year (e.g., Humboldt Current in winter–spring; Chavez et al. 2008). In this sense, the case of Galápagos Islands highlights the limitations of modeling a 3D environment in two dimensions. This model limitation may also be an underlying cause of connectivity underprediction between the Galápagos Islands and the Northeast Pacific subpopulation, which is relevant considering *N. cepedianus*' anti-tropical distribution (Ludt 2021). The advent of promising tools for 3D environmental niche modeling in recent years (Bentlage et al. 2013) may provide avenues for better understanding habitat use of other demersal species widely distributed across the vertical dimension.

Dispersal corridors, population connectivity, and absence from the North Atlantic

Based on the modeling approach, temperate coasts in the North Atlantic represent suitable habitats for *N. cepedianus* (Fig. 5, binary output in Supporting Information Fig. S11). So after the genus *Notorynchus* disappeared from the North Atlantic (~ 4 Mya) what has prevented *N. cepedianus* re-establishing in the suitable North Atlantic coastal habitats? Information on the species to date suggests that warmer, colder and deeper waters act as barriers to dispersal, and therefore the nearest subpopulations that could colonize the North Atlantic from the South Atlantic are likely blocked by the equatorial barrier. A combination of great distances and lack of seamount/knoll

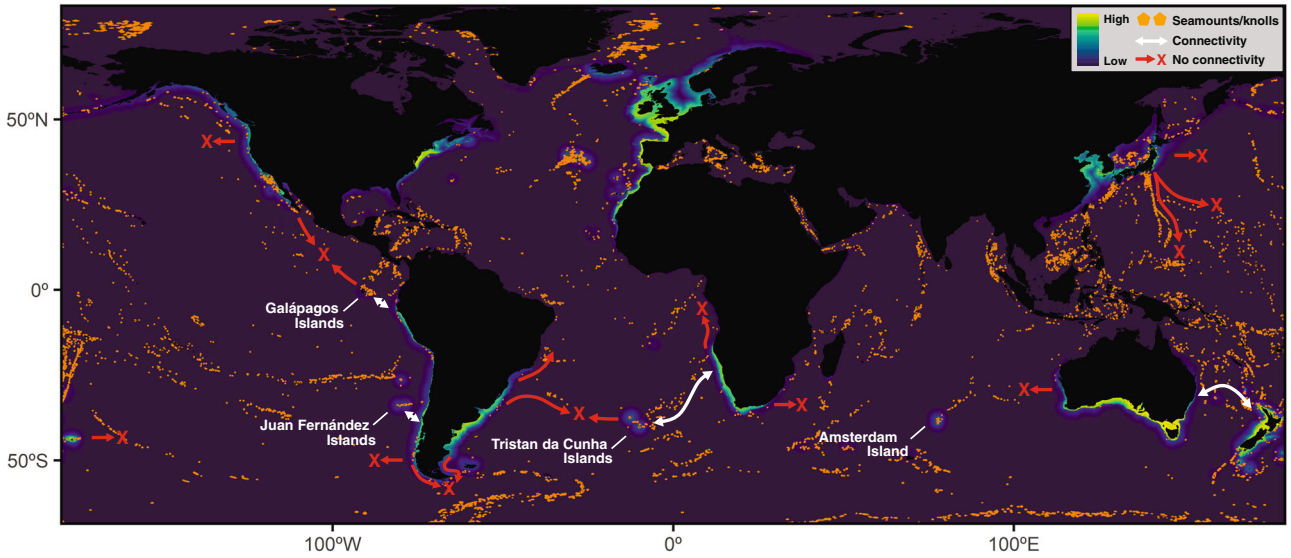

Fig. 5. Global continuous habitat suitability for *Notorynchus cepedianus* and relevant (< 600 m deep) seamount and knoll data (base polygons). Connectivity and no connectivity refer to the plausibility of potential subpopulation connectivity through seamounts and knolls based on dispersal simulations. No connectivity outside connectivity hotspots refers to physiological limits, transoceanic distances or lack of seamount continuity. Offshore archipelagos relevant to the study are indicated.

continuity from South Atlantic subpopulations to North Atlantic habitats could be a factor, for example, seamount/knoll distribution data suggests no connectivity between the two regions via deeper and cooler waters within the known depth range of the species (Fig. 5). However, genetic connectivity appears to be evident across the equator between California and Peru (Schmidt-Roach et al. 2021), where no connectivity is predicted via seamounts/knolls across the equator (between Northeast and Southeast Pacific; Fig. 5). As in the North Atlantic, connections between other suitable regions are not expected. Connectivity between Oceania and Northwest Pacific is considered unlikely because of vast distances separating the two regions (> 8000 km). *N. cepedianus* subpopulation(s) in the Northwest Pacific is likely the most isolated in the world.

Seamount and knoll distribution and dispersal simulations suggested different degrees of connectivity between known occupied regions. Patterns indicate connectivity within major oceanic basins, namely South Atlantic (connection Tristan da Cunha Islands and Southeast Atlantic), Oceania in Southwest Pacific (connection southern Australia and New Zealand), and Eastern Pacific (connection Southeast Pacific and Galápagos Islands). In theory, there are seamounts/knolls connecting the west and east Pacific, but the large distance across the ocean basin likely prevents any connection. The Indian Ocean lacks seamount/knoll stepping stones, predicted suitable habitats (except Amsterdam/Saint-Paul Islands) and, besides the southwest corner of Australia (the very edge of *N. cepedianus* distribution in this region), has no confirmed presence of *N. cepedianus*. These findings coincide with those by Schmidt-Roach et al. (2021), who examined patterns of genetic structure (using mitochondrial and nuclear DNA) in the most well-known *N. cepedianus* subpopulations across the world. Genetic connectivity was evident between southern Australia and New Zealand (Oceania), United States, and Peru (Eastern Pacific), and Argentina and South Africa (South Atlantic), but not between Oceania, Eastern Pacific or the South Atlantic (Schmidt-Roach et al. 2021). Schmidt-Roach et al. (2021) proposed a historical divergence and subsequent isolation between Oceania, Eastern Pacific, and South Atlantic regions, which initiated near 0.55 Mya ago in the mid Pleistocene. We hypothesize that such isolation is currently maintained because of the lack of suitable coastal and seamount/knoll (up to 600 m) dispersal corridors. In addition, genetic isolation in *N. cepedianus* could explain the subpopulation niche differentiation between Southwest Atlantic and southern Australia found in this study.

Within each major oceanic region, connectivity between suitable areas could be facilitated by underwater seamount/knoll ranges. In the South Atlantic, seamounts may function as a bridge between Tristan da Cunha Islands and Southeast Atlantic subpopulations. In the Eastern Pacific, genetic connectivity between Northeast and Southeast Pacific regions across the tropics may be explained by long-distance dispersal through deep channels (Schmidt-Roach et al. 2021). However, the mapping in the current study did not support connectivity via seamounts between the Northeast and Southeast Pacific regions, suggesting other oceanographic features like cold currents may play a role in facilitating *N. cepedianus* dispersal through the equatorial barrier. In the Southeast Pacific, dispersal to Juan Fernández Islands (Chile) is also expected due to proximity to the continent and availability of seamount/

knoll providing stepping stone pathways (Fig. 5). The recent increase in reports of *N. cepedianus* from Chile and Peru (Bustamante et al. 2021; Schmidt-Roach et al. 2021) suggests the existence of a subpopulation(s) in the region, but as with most other regions, further work is needed to understand connectivity within the Southeast Pacific (Schmidt-Roach et al. 2021). As discussed by Schmidt-Roach et al. (2021), further work that includes more sensitive genetic markers (Larson et al. 2015) and tracking methods are needed to elucidate gene flow within regions.

Data availability statement

Most presence records from this study are open and available in the Supporting Information. The code to perform all analyses can be accessed at https://github.com/Agustindewy/Sevengill_shark_global

References

Aiello-Lammens, M. E., R. A. Boria, A. Radosavljevic, B. Vilela, and R. P. Anderson. 2015. spThin: An R package for spatial thinning of species occurrence records for use in ecological niche models. Ecography **38**: 541–545. doi:10.1111/ecog.01132

Anderson, O. F., N. Bagley, R. J. Hurst, M. P. Francis, M. R. Clark, and P. McMillan. 1998. Atlas of New Zealand fish and squid distributions from research bottom trawls. NIWA Tech. Rep. **42**: 300.

Araújo, M. B., and others. 2019. Standards for distribution models in biodiversity assessments. Sci. Adv. **5**: 1–12. doi:10.1126/sciadv.aat4858

Assis, J., L. Tyberghein, S. Bosch, H. Verbruggen, E. A. Serrão, and O. De Clerck. 2018. Bio-ORACLE v2.0: Extending marine data layers for bioclimatic modelling. Glob. Ecol. Biogeogr. **27**: 277–284. doi:10.1111/geb.12693

Barbini, S. A., L. O. Lucifora, and D. E. Figueroa. 2015. Using opportunistic records from a recreational fishing magazine to assess population trends of sharks. Can. J. Fish. Aquat. Sci. **72**: 1853–1859. doi:10.1139/cjfas-2015-0087

Barnett, A., and J. M. Semmens. 2012. Sequential movement into coastal habitats and high spatial overlap of predator and prey suggest high predation pressure in protected areas. Oikos **121**: 882–890. doi:10.1111/j.1600-0706.2011.20000.x

Barnett, A., K. G. Abrantes, J. D. Stevens, B. D. Bruce, and J. M. Semmens. 2010 *a*. Fine-scale movements of the Broadnose Sevengill shark and its main prey, the gummy shark. PLoS One **5**: 15464. doi:10.1371/journal.pone.0015464

Barnett, A., J. D. Stevens, S. D. Frusher, and J. M. Semmens. 2010 *b*. Seasonal occurrence and population structure of the broadnose sevengill shark *Notorynchus cepedianus* in coastal habitats of south-east Tasmania. J. Fish Biol. **77**: 1688–1701. doi:10.1111/j.1095-8649.2010.02810.x

Barnett, A., K. G. Abrantes, J. D. Stevens, and J. M. Semmens. 2011. Site fidelity and sex-specific migration in a mobile apex predator: Implications for conservation and ecosystem dynamics. Anim. Behav. **81**: 1039–1048. doi:10.1016/j.anbehav.2011.02.011

Barnett, A., J. M. Braccini, C. A. Awruch, and D. A. Ebert. 2012. An overview on the role of Hexanchiformes in marine ecosystems: Biology, ecology and conservation status of a primitive order of modern sharks. J. Fish Biol. **80**: 966–990. doi:10.1111/j.1095-8649.2012.03242.x

Barnett, A., M. Braccini, C. L. Dudgeon, N. L. Payne, K. G. Abrantes, M. Sheaves, and E. P. Snelling. 2017. The utility of bioenergetics modelling in quantifying predation rates of marine apex predators: Ecological and fisheries implications. Sci. Rep. **7**: 1–10. doi:10.1038/s41598-017-13388-y

Battini, N., N. Farías, C. B. Giachetti, E. Schwindt, and A. Bortolus. 2019. Staying ahead of invaders: Using species distribution modeling to predict alien species' potential niche shifts. Mar. Ecol. Prog. Ser. **612**: 127–140. doi:10.3354/meps12878

Benavides, M. T., and others. 2011. Phylogeography of the copper shark (*Carcharhinus brachyurus*) in the southern hemisphere: Implications for the conservation of a coastal apex predator. Mar. Freshw. Res. **62**: 861–869. doi:10.1071/MF10236

Bentlage, B., A. T. Peterson, N. Barve, and P. Cartwright. 2013. Plumbing the depths: Extending ecological niche modelling and species distribution modelling in three dimensions. Glob. Ecol. Biogeogr. **22**: 952–961. doi:10.1111/geb.12049

Bester-van der Merwe, A. E., D. Bitalo, J. M. Cuevas, J. Ovenden, S. Hernández, C. Da Silva, M. McCord, and R. Roodt-Wilding. 2017. Population genetics of Southern Hemisphere tope shark (*Galeorhinus galeus*): Intercontinental divergence and constrained gene flow at different geographical scales. PLoS One **12**: 1–20. doi:10.1371/journal.pone.0184481

Braccini, M., B. Molony, and N. Blay. 2020. Patterns in abundance and size of sharks in northwestern Australia: Cause for optimism. ICES J. Mar. Sci. **77**: 72–82. doi:10.1093/icesjms/fsz187

Bradley, M., I. Nagelkerken, R. Baker, and M. Sheaves. 2020. Context dependence: A conceptual approach for understanding the habitat relationships of coastal marine Fauna. Bioscience **XX**: 1–19. doi:10.1093/biosci/biaa100

Buglass, S., S. Nagy, D. Ebert, P. Sepa, A. Turchik, K. L. C. Bell, F. Rivera, and J. Giddens. 2020. First records of the sevengilled *Notorynchus cepedianus* and six-gilled *Hexanchus griseus* sharks (Chondrichthyes: Hexanchiformes: Hexanchidae) found in the Galápagos Marine Reserve. J. Fish Biol. **97**: 926–929. doi:10.1111/jfb.14447

Bustamante, C., A. M. García-Cegarra, and C. Vargas-Caro. 2021. Observations of coastal aggregations of the broadnose sevengill shark (*Notorynchus cepedianus*) in

Chilean waters. J. Fish Biol. **98**: 870–873. doi:10.1111/jfb.14591

Caselle, J. E., S. L. Hamilton, K. Davis, C. D. H. Thompson, A. Turchik, R. Jenkinson, D. Simpson, and E. Sala. 2018. First quantification of subtidal community structure at Tristan da Cunha islands in the remote South Atlantic: From kelp forests to the deep sea. PLos One **13**: e0195167.

Chavez, F. P., A. Bertrand, R. Guevara-Carrasco, P. Soler, and J. Csirke. 2008. The northern Humboldt Current System: Brief history, present status and a view towards the future. Prog. Oceanogr. **79**: 95–105. doi:10.1016/j.pocean.2008.10.012

Cobos, M. E., L. Jiménez, C. Nuñez-Penichet, D. Romero-Alvarez, and M. Simoes. 2018. Sample data and training modules for cleaning biodiversity information. Biodivers. Inf. **13**: 49–50. doi:10.17161/bi.v13i0.7600

Cobos, M. E., A. T. Peterson, L. Osorio-Olvera, and D. Jiménez-García. 2019 *a*. An exhaustive analysis of heuristic methods for variable selection in ecological niche modeling and species distribution modeling. Ecol. Inf. **53**: 100983. doi:10.1016/j.ecoinf.2019.100983

Cobos, M. E., T. A. Peterson, N. Barve, and L. Osorio-Olvera. 2019 *b*. kuenm: An R package for detailed development of ecological niche models using Maxent. PeerJ **7**: 1–15. doi:10.7717/peerj.6281

Cobos, M. E., L. Osorio-Olvera, J. Soberón, A. T. Peterson, V. Barve, and N. Barve. 2020. ellipsenm: An R package for ecological niche's characterization using ellipsoids. GitHub repository. Available from https://github.com/marlonecobos/ellipsenm

Dawson, M. N. 2016. Island and Island-like marine environments. Glob. Ecol. Biogeogr. **25**: 831–846. doi:10.1111/geb.12314

De Wysiecki, A. M., and others. 2020. Using temporally explicit habitat suitability models to infer the migratory pattern of a large mobile shark. Can. J. Fish. Aquat. Sci. **77**: 1529–1539. doi:10.1139/cjfas-2020-0036

Dormann, C. F., and others. 2013. Collinearity: A review of methods to deal with it and a simulation study evaluating their performance. Ecography **36**: 27–46. doi:10.1111/j.1600-0587.2012.07348.x

Ebert, D. A. 1989. Life history of the sevengill shark, *Notorynchus cepedianus* Peron, in two northern California bays. Calif. Dep. Fish Game **75**: 102–112.

Ebert, D. A. 1996. Biology of the sevengill shark *Notorynchus cepedianus* (Peron, 1807) in the temperate coastal waters of Southern Africa. South Afr. J. Mar. Sci. **17**: 93–103. doi:10.2989/025776196784158545

Ebert, D. A., H. C. Ho, W. T. White, and M. R. De Carvalho. 2013. Introduction to the systematics and biodiversity of sharks, rays, and chimaeras (Chondrichthyes) of Taiwan. Zootaxa **3752**: 5–19. doi:10.11646/zootaxa.3752.1.3

Engelbrecht, T. M., A. A. Kock, M. J. O'Riain, B. Q. Mann, S. W. Dunlop, and A. Barnett. 2020. Movements and growth rates of the broadnose sevengill shark *Notorynchus cepedianus* in southern Africa: Results from a long-term cooperative tagging programme. Afr. J. Mar. Sci. **42**: 247–259. doi:10.2989/1814232X.2020.1802776

Finucci, B., A. Barnett, J. Cheok, C. F. Cotton, D. W. Kulka, F. C. Neat, N. Pacoureau, C. L. Rigby, S. Tanaka, and T. I. Walker. 2020. *Notorynchus cepedianus*. The IUCN red list of threatened species, e.T39324A2896914. doi:10.2305/IUCN.UK.2020-3.RLTS.T39324A2896914.en

Franco, B. C., V. Combes, and V. González Carman. 2020. Subsurface Ocean warming hotspots and potential impacts on marine species: The Southwest South Atlantic Ocean case study. Front. Mar. Sci. **7**: 1–13. doi:10.3389/fmars.2020.563394

Froese, R., and D. Pauly. 2019. *Notorynchus cepedianus*. FishBase. World Wide Web electronic publication.

Frusher, S. D., and others. 2014. The short history of research in a marine climate change hotspot: From anecdote to adaptation in south-east Australia. Rev. Fish Biol. Fish. **24**: 593–611. doi:10.1007/s11160-013-9325-7

GBIF. 2020. GBIF occurrence download. doi:10.15468/dl.y7kyfq

Hijmans, R. J. 2021. raster: Geographic Data Analysis and Modeling. R package version 3.4-13. https://CRAN.R-project.org/package=raster

Hirschfeld, M., C. Dudgeon, M. Sheaves, and A. Barnett. 2021. Barriers in a sea of elasmobranchs: From fishing for populations to testing hypotheses in population genetics. Glob. Ecol. Biogeogr. **30**: 2147–2163. doi:10.1111/geb.13379

Hirzel, A. H., G. Le Lay, V. Helfer, C. Randin, and A. Guisan. 2006. Evaluating the ability of habitat suitability models to predict species presences. Ecol. Model. **199**: 142–152. doi:10.1016/j.ecolmodel.2006.05.017

Hortal, J., A. Jiménez-Valverde, J. F. Gómez, J. M. Lobo, and A. Baselga. 2008. Historical bias in biodiversity inventories affects the observed environmental niche of the species. Oikos **117**: 847–858. doi:10.1111/j.0030-1299.2008.16434.x

Hutchinson, G. E. 1957. Concluding remarks. Cold Spring Harb. Symp. Quant. Biol. **22**: 415–427. doi:10.1101/sqb.1957.022.01.039

Ingenloff, K., and A. T. Peterson. 2021. Incorporating time into the traditional correlational distributional modelling framework: A proof-of-concept using the Wood Thrush *Hylocichla mustelina*. Methods Ecol. Evol. **12**: 311–321. doi:10.1111/2041-210X.13523

Irigoyen, A., and G. Trobbiani. 2016. Depletion of trophy large-sized sharks populations of the Argentinean coast, South-Western Atlantic: Insights from fishers' knowledge. Neotrop. Ichthyol. **14**: e150081. doi:10.1590/1982-0224-20150081

Irigoyen, A. J., A. M. De Wysiecki, G. Trobbiani, N. Bovcon, C. A. Awruch, F. Argemi, and A. J. Jaureguizar. 2018.

Habitat use, seasonality and demography of an apex predator: Sevengill shark *Notorynchus cepedianus* in Northern Patagonia. Mar. Ecol. Prog. Ser. **603**: 147–160. doi:10.3354/meps12715

Kass, J. M., R. Muscarella, P. J. Galante, C. L. Bohl, G. E. Pinilla-Buitrago, R. A. Boria, M. Soley-Guardia, and R. P. Anderson. 2021. ENMeval 2.0: Redesigned for customizable and reproducible modeling of species' niches and distributions. Methods Ecol. Evol. **12**: 1602–1608. doi:10.1111/2041-210X.13628

Larson, S., D. Farrer, D. Lowry, and D. A. Ebert. 2015. Preliminary observations of population genetics and relatedness of the broadnose sevengill shark, *Notorynchus cepedianus*, in two northeast Pacific estuaries. PLoS One **10**: e0129278. doi:10.1371/journal.pone.0129278

Leroy, B., R. Delsol, B. Hugueny, C. N. Meynard, C. Barhoumi, M. Barbet-Massin, and C. Bellard. 2018. Without quality presence–absence data, discrimination metrics such as TSS can be misleading measures of model performance. J. Biogeogr. **45**: 1994–2002. doi:10.1111/jbi.13402

Lewis, R., S. Dawson, and W. Rayment. 2020. Estimating population parameters of broadnose sevengill sharks (*Notorynchus cepedianus*) using photo identification capture-recapture. J. Fish Biol. **97**: 987–995. doi:10.1111/jfb.14453

Lucifora, L. O., R. C. Menni, and A. H. Escalante. 2005. Reproduction, abundance and feeding habits of the broadnose sevengill shark *Notorynchus cepedianus* in north Patagonia, Argentina. Mar. Ecol. Prog. Ser **289**: 237–244. doi:10.3354/meps289237

Ludt, W. B. 2021. Missing in the middle: A review of equatorially disjunct marine taxa. Front. Mar. Sci. **8**: 660984. doi:10.3389/fmars.2021.660984

MacLeod, C. D. 2009. Global climate change, range changes and potential implications for the conservation of marine cetaceans: A review and synthesis. Endanger. Spec. Res. **7**: 125–136. doi:10.3354/esr00197

Maisey, J. G. 2012. What is an "elasmobranch"? The impact of palaeontology in understanding elasmobranch phylogeny and evolution. J. Fish Biol. **80**: 918–951. doi:10.1111/j.1095-8649.2012.03245.x

Melo-Merino, S. M., H. Reyes-Bonilla, and A. Lira-Noriega. 2020. Ecological niche models and species distribution models in marine environments: A literature review and spatial analysis of evidence. Ecol. Model. **415**: 108837. doi:10.1016/j.ecolmodel.2019.108837

Muscarella, R., P. J. Galante, M. Soley-Guardia, R. A. Boria, J. M. Kass, M. Uriarte, and R. P. Anderson. 2014. ENMeval: An R package for conducting spatially independent evaluations and estimating optimal model complexity for Maxent ecological niche models. Methods Ecol. Evol. **5**: 1198–1205. doi:10.1111/2041-210x.12261

Niella, Y., P. Butcher, B. Holmes, A. Barnett, and R. Harcourt. 2022. Forecasting intraspecific changes in distribution of a wide-ranging marine predator under climate change. Oecologia **198**: 111–124. doi:10.1007/s00442-021-05075-7

Nuñez-Penichet, C., and others. 2021. Geographic potential of the world's largest hornet, *Vespa mandarinia* Smith (Hymenoptera: Vespidae), worldwide and particularly in North America. PeerJ **9**: e10690. doi:10.7717/peerj.10690

OBIS. 2020. Distribution records of *Notorynchus cepedianus* (Péron, 1807) [Dataset]. Ocean Biodiversity Information System, Intergovernmental Oceanographic Commission of UNESCO. Available from www.iobis.org

Osorio-Olvera L., and J. Soberón. 2020. bam: Species distribution models in the light of the BAM theory. Available from https://github.com/luismurao/bam

Owens, H. L., A. C. Bentley, and A. T. Peterson. 2012. Predicting suitable environments and potential occurrences for coelacanths (*Latimeria* spp.). Biodivers. Conserv. **21**: 577–587. doi:10.1007/s10531-011-0202-1

Owens, H. L., and others. 2013. Constraints on interpretation of ecological niche models by limited environmental ranges on calibration areas. Ecol. Model. **263**: 10–18. doi:10.1016/j.ecolmodel.2013.04.011

Peterson, A. T., J. Soberón, R. G. Pearson, R. P. Anderson, E. Martínez-Meyer, M. Nakamura, and M. B. Araújo. 2011. Ecological niches and geographic distributions. Princeton Univ. Press.

Phillips, S. J., R. P. Anderson, and R. E. Schapire. 2006. Maximum entropy modeling of species geographic distributions. Ecol. Model. **190**: 231–259. doi:10.1016/j.ecolmodel.2005.03.026

R Core Team. 2021. R: A language and environment for statistical computing. R Foundation for Statistical Computing.

Reinecke, T., M. Balsberger, B. Beaury, and J. Pollerspöck. 2014. The elasmobranch fauna of the Thalberg Beds, early Egerian (Chattian, Oligocene), in the Subalpine Molasse Basin near Siegsdorf, Bavaria, Germany. Palaeontos **26**: 3–129.

Schlaff, A. M., M. R. Heupel, and C. A. Simpfendorfer. 2014. Influence of environmental factors on shark and ray movement, behaviour and habitat use: A review. Rev. Fish Biol. Fish **1089–1103**: 1089–1103. doi:10.1007/s11160-014-9364-8

Schmidt-Roach, A. C. J., and others. 2021. Evidence of historical isolation and genetic structuring among broadnose sevengill sharks (*Notorynchus cepedianus*) from the world's major oceanic regions. Rev. Fish Biol. Fish. **31**: 433–447. doi:10.1007/s11160-021-09651-1

Smart, P. J. 2001. An underscribed late Cretaceous *Notorynchus* tooth (Chondrichthyes, vertebrata) from the English Chalk. Proc. Geol. Assoc. **112**: 59–62. doi:10.1016/S0016-7878(01)80049-3

Soberón, J., and A. T. Peterson. 2005. Interpretation of models of fundamental ecological niches and species' distributional areas. Biodivers. Inf. **2**: 1–13. doi:10.17161/bi.v2i0.4

Soberón, J., and M. Nakamura. 2009. Niches and distributional areas: Concepts, methods, and assumptions. Proc. Natl.

Acad. Sci. USA **106**: 19644–19650. doi:10.1073/pnas.0901637106

Stehfest, K. M., T. A. Patterson, A. Barnett, and J. M. Semmens. 2014. Intraspecific differences in movement, dive behavior and vertical habitat preferences of a key marine apex predator. Mar. Ecol. Prog. Ser. **495**: 249–262. doi:10.3354/meps10563

Sunday, J. M., and others. 2015. Species traits and climate velocity explain geographic range shifts in an ocean-warming hotspot. Ecol. Lett. **18**: 944–953. doi:10.1111/ele.12474

Tanaka, K., and others. 2013. Evolutionary relations of hexanchiformes deep-sea sharks elucidated by whole mitochondrial genome sequences. Biomed. Res. Int. **2013**: 1–11. doi:10.1155/2013/147064

Valavi, R., J. Elith, J. J. Lahoz-Monfort, and G. Guillera-Arroita. 2019. blockCV: An r package for generating spatially or environmentally separated folds for k-fold cross-validation of species distribution models. Methods Ecol. Evol. **10**: 225–232. doi:10.1111/2041-210X.13107

Van Aelst, S., and P. Rousseeuw. 2009. Minimum volume ellipsoid. Wiley Interdiscip. Rev. Comput. Stat. **1**: 71–82. doi:10.1002/wics.19

Varela, S., R. P. Anderson, R. García-Valdés, and F. Fernández-González. 2014. Environmental filters reduce the effects of sampling bias and improve predictions of ecological niche models. Ecography **37**: 1084–1091. doi:10.1111/j.1600-0587.2013.00441.x

Wessel, P., and W. H. F. Smith. 1996. A global, self-consistent, hierarchical, high-resolution shoreline database. J. Geophys. Res. B Solid Earth **101**: 8741–8743. doi:10.1029/96jb00104

Williams, G. D., K. S. Andrews, S. L. Katz, M. L. Moser, N. Tolimieri, D. A. Farrer, and P. S. Levin. 2012. Scale and pattern of broadnose sevengill shark *Notorynchus cepedianus* movement in estuarine embayments. J. Fish Biol. **80**: 1380–1400. doi:10.1111/j.1095-8649.2011.03179.x

Yesson, C., M. R. Clark, M. L. Taylor, and A. D. Rogers. 2011. The global distribution of seamounts based on 30 arc seconds bathymetry data. Deep. Res. Part I Oceanogr. Res. Pap **58**: 442–453. doi:10.1016/j.dsr.2011.02.004

Zurell, D., and others. 2020. A standard protocol for reporting species distribution models. Ecography **43**: 1261–1277. doi:10.1111/ecog.04960

Acknowledgments

This study was developed in the context of Agustin M. De Wysiecki' doctoral thesis supported by a scholarship by Consejo Nacional de Investigaciones Científicas y Técnicas (CONICET, Argentina). The authors give special thanks to Marlon E. Cobos and Noela Sanchez-Carnero who provided cornerstone recommendations and comments on an earlier draft of this manuscript. Jorge H. Colonello, Instituto Nacional de Investigación y Desarrollo Pesquero (INIDEP, Argentina) and Australian Fishery Management Authority (AFMA) kindly provided presence data. INIDEP assigned the internal No 2265 to this contribution. Thanks to Kátya G. Abrantes who revised and improved the last version of this manuscript. Agustin De Wysiecki thanks Adriana Ruggiero and students for the opportunity to discuss this study in the 2020 postgraduate course "Biogeografía" at Universidad del Comahue (UNCo, Argentina). Open access publishing facilitated by James Cook University, as part of the Wiley - James Cook University agreement via the Council of Australian University Librarians.

Conflict of Interest

None declared.

Submitted 30 July 2021
Revised 18 November 2021
Accepted 22 May 2022

Associate editor: Bingzhang Chen